# Evaluation of the Role of Pores during Strength Testing in Compacts Made from Different Particle Size Fractions of Sucrose

Helena NICKLASSON[a] and Fridrun PODCZECK*,[b]

[a] *Department of Pharmacy, Uppsala University; SE-75123 Uppsala, Sweden: and* [b] *Division of Pharmacy, Chemistry and Biomedical Sciences, Sunderland University; Sunderland SR1 3SD, U.K.* Received June 16, 2006; accepted October 13, 2006

**The purpose of this study was to investigate the role of pores in the fracture of circular compacts and to predict compact properties and critical crack lengths. Four different particle size fractions of sucrose, ranging from 20 to 500 $\mu$m, were compressed into circular discs (*i.e.* flat tablets) and rectangular beam specimens of porosity between 30 and 14%. Modelling of the relationship between the tensile strength of the circular discs and the compact porosity indicated extensive fragmentation during compaction for particles in the size range of 250—500 $\mu$m, accompanied by a change in densification mechanism for very coarse particles (355—500 $\mu$m). When determining the critical stress intensity factor from rectangular single edge notched beam specimens by 3-point bending, an apparent influence of particle size on the values could be seen, whereby here the results indicated that the critical particle size for fragmentation to occur is about 20—40 $\mu$m. It was possible to predict the critical stress intensity factor of the compacts from the median pore size and the tensile strength of the circular disc specimens by interpolation of the critical crack length for propagation to occur. The results indicated that for sucrose compacts regardless of their porosity, the pores themselves acted as stress concentrators, not as sharp cracks. For sucrose compacts, crack propagation hence proceeds most likely along grain boundaries.**

**Key words** fracture mechanics; median pore size; tablet tensile strength; sucrose

The mechanical strength of pharmaceutical compacts is an important in-process control parameter to ensure that tablets have sufficient strength to withstand handling during production, transport and use.[1)] The introduction of the "Brazilian test"[2)] into the pharmaceutical sciences by Fell and Newton[3,4)] has enabled a fundamental understanding of the stresses involved in the breaking of compacts and provided a tool to characterise the mechanical properties of the compacted materials. The failure of such compacts under load is undoubtedly a matter of fracture mechanics *i.e.* crack propagation. However, while the interpretation of the measured failure properties on the basis of modern linear elastic fracture mechanics is well understood, the prediction of the failure properties of such specimens would be desirable yet is much more difficult. In particular, the role of pores inside the specimens and their size and shape distribution in the fracture process is not clear. In this paper, the role of pores in the fracture of circular disc specimens made from sucrose of various particle size fractions has been studied and a prediction of compact properties and critical crack lengths was attempted.

## Experimental

**Materials** Crystalline sucrose (Svenskt socker AB, Sweden) was used for the experiments. To obtain the two coarse particle fractions (250—355, 355—500 $\mu$m), dry sieving of the raw material was undertaken (Retsch laboratory sieves, Haan, Germany). In order to obtain the finer size fractions (20—40, 40—80 $\mu$m) the raw material was milled in a pin disc mill (Alpine 63C, Alpine AG, Augsburg, Germany) and classified using air classification (Alpine 100 MZR, Alpine AG, Augsburg, Germany). The particle size distribution of the individual fractions was determined microscopically. All fractions showed a mono-modal, continuous distribution function, slightly skewed to the left.

**Methods** Compacts in the shape of a circular disc of 11 mm diameter and rectangular beams of 24×13 mm were made at four and five levels of porosity, respectively, adjusting the powder weight and keeping the compact thickness constant at 3.8 mm. For the circular tablets the compaction pressures used were 75, 100, 125 and 150 MPa, and the resulting porosities are reported in Table 1. For the rectangular beams compaction pressures between 70 and 170 MPa were used, increasing the pressure in steps of 25 MPa. The porosities achieved can be obtained from Fig. 2. A physical testing machine (Model TT, Instron, High Wycombe, U.K.) was employed using a cross-head speed of 1 mm/min. For the lowest porosity levels, a manually operated hydraulic press (Specac 15,000, Birmingham, U.K.) was used. In all cases the compacts were left under pressure for 3 min to reduce relaxation after ejection, which could have a larger influence on the final compact thickness. The die walls and punches were cleaned, polished and lubricated with magnesium stearate powder prior to each new compact being made. Nine beams and at least six tablets were made at each level of porosity. The compacts were stored at room temperature at approximately 35% relative humidity for 3 d prior to testing.

Each compact was weighed to ±0.0001 g on an electronic balance (Mettler AE 160, Zürich, Switzerland). The compact thickness and the beam width were measured to 0.001 mm using an electronic calliper (Moore & Wright, Sheffield, U.K.), and the beam length was measured to 0.01 mm using an electronic micrometer (Digimatic, Mitutoyo, Tokyo, Japan).

The tablet pore size distributions were determined by mercury intrusion porosimetry (AutoPore III, Micromeritics, U.S.A.) by analysing the relationship between the mercury intrusion volume and the intrusion pressure. Intrusion pressures between 1.5 and 60000 psia were used. The pore size corresponding to the intrusion pressures applied were calculated assuming circular pore openings and a surface tension of mercury of 485 mN/m. The contact angle between mercury and sucrose was measured using a 1501 Contact Anglometer (Micromeritics, U.S.A.) and found to be 101.5°. The median pore size was calculated from the intruded mercury volumes at each pressure level. The maximum pore size was calculated from the lowest pressure, at which the intruded mercury volume deviated from the base line. The volume specific surface area of the particle fragments after compaction was determined from the tablets using air pycnometry. A full account of the methodology and data processing has been reported by Olsson and Nyström[5)] and by Alderborn *et al.*[6)]

The tablet tensile strength was determined using a CT-5 strength tester (Engineering Systems, Nottingham, U.K.).

To evaluate the critical stress intensity factor, a crack was introduced in the middle of the upper face of each beam specimen using a Japanese pull-saw with a thickness of the blade of 300 $\mu$m (Handiwork micro saw, Takagi, Japan). The depth of the cracks was measured using an image analyser (Seescan Solitaire 512, Cambridge, U.K.) attached to a CCD-4 b/w-camera (Rengo Co., Toyohashi, Japan) and an Olympus BH-2 microscope (Olympus Co., Tokyo, Japan). The magnification was chosen so that the measuring error did not exceed ±7 $\mu$m.

The cracked specimens were loaded in 3-point bending (CT-5, Engineering Systems, Nottingham, U.K.) with the crack facing downwards. The span between the centres of the lower support rolls was 18 mm. A 5 kg load cell

* To whom correspondence should be addressed. e-mail: fridrun.podczeck@sunderland.ac.uk 

Table 1. Data Obtained from Round Compacted Disk Specimens (Arithmetic Mean and Standard Deviation of $n$ Observations)

| Fraction | Porosity ($n$=6) | Pore size ($\mu$m; $n$=3) | | Tensile strength (MPa; $n$=6) |
|---|---|---|---|---|
| | | Median | Maximum | |
| 1 (20—40 $\mu$m) | 0.309±0.005 | 0.61±0.05 | 0.76±0.02 | 0.55±0.07 |
| | 0.242±0.009 | 0.45±0.07 | 0.62±0.11 | 1.04±0.10 |
| | 0.211±0.003 | 0.31±0.04 | 0.43±0.02 | 1.32±0.06 |
| | 0.207±0.003 | 0.28±0.02 | 0.34±0.05 | 1.31±0.11 |
| 2 (40—80 $\mu$m) | 0.268±0.009 | 0.72±0.08 | 0.97±0.02 | 0.63±0.04 |
| | 0.226±0.005 | 0.47±0.06 | 0.70±0.08 | 0.85±0.08 |
| | 0.193±0.003 | 0.39±0.02 | 0.61±0.14 | 1.06±0.09 |
| | 0.180±0.009 | 0.31±0.02 | 0.44±0.05 | 1.47±0.13 |
| 3 (250—355 $\mu$m) | 0.198±0.009 | 0.91±0.44 | 4.61±1.16 | 0.40±0.01 |
| | 0.163±0.015 | 0.56±0.01 | 2.84±0.10 | 0.57±0.02 |
| | 0.143±0.032 | 0.42±0.04 | 3.14±0.35 | 0.61±0.04 |
| | 0.141±0.002 | 0.35±0.01 | 1.28±0.12 | 0.87±0.07 |
| 4 (355—500 $\mu$m) | 0.207±0.011 | 1.37±0.04 | 7.57±0.67 | 0.38±0.03 |
| | 0.175±0.008 | 0.91±0.11 | 3.29±0.04 | 0.50±0.02 |
| | 0.152±0.003 | 0.57±0.06 | 2.69±0.16 | 0.60±0.05 |
| | 0.143±0.008 | 0.42±0.06 | 2.70±0.30 | 0.83±0.05 |

Table 2. Model Data for Tensile Strength ($\sigma_f$) as a Function of Tablet Porosity, and Critical Stress Intensity Factor at Zero Porosity ($K_{IC}^0$)

| Fraction | Model data ($\sigma_f$=$f$(porosity)) | | | | $K_{IC}^0$ (MPa m$^{0.5}$) |
|---|---|---|---|---|---|
| | Function | Parameters | | | |
| 1 (20—40 $\mu$m) | Linear | $\sigma_0$=2.889 | $b$=−0.076 | | 0.61±0.11 |
| 2 (40—80 $\mu$m) | Exponential | $\sigma_0$=6.563 | $b$=−0.089 | | 0.35±0.03 |
| 3 (250—355 $\mu$m) | (Exponential | $\sigma_0$=3.367 | $b$=−0.108) | | 0.31±0.03 |
| 4 (355—500 $\mu$m) | Quadratic | $\sigma_0$=5.285 | $b_1$=−0.488 | $b_2$=0.012 | 0.28±0.02 |

$\sigma_0$, tensile strength at zero porosity; $b, b_1, b_2$, model dependent constants.

was employed and the maximum breaking load was read. The beams were tested at a constant strain rate of 1 mm/min. The force was also recorded as a function of displacement (Servogor 120, BBC Goerz Metrawatt, U.K.) to monitor the fracture behaviour. In those cases, where small deviations from instable crack growth were observed, the maximum breaking load was corrected as described by Brown and Srawley.[7] The critical stress intensity factor was determined for each beam as described by Podczeck,[8] and zero-porosity value approximation was undertaken on the basis of Spriggs' equation.[9] The required minimum crack depth to obtain a crack, which is large enough to control the fracture process, was calibrated by plotting the critical stress intensity factor as a function of crack depth as suggested by Podczeck.[8]

All calculations were carried out using SPSS 9.0 (SPSS Inc., Woking, U.K.).

## Results and Discussion

**Tablet Tensile Strength** The tablet tensile strength and accompanying results (porosity and pore size values) are listed in Table 1. The data available allowed an estimate of the zero tensile strength, which is provided in Table 2 (residual analysis: RMS<5% and $R^2$>0.93, except for size fraction 3, where no satisfactory fitting algorithm could be found). In the literature, strength data are mostly related to porosity *via* an exponential function as suggested first by Ryshkewitch[10] and Duckworth.[11] The better fit of the linear approximation for the smallest particle size fraction might simply be due to a lack of values closer to zero porosity. Power functions were also reported in the literature,[12] and hence the results obtained for the largest particle size fraction might be a true reflection of a change in densification mechanism due to the coarse particle size.

Knudsen[13] suggested relating the tensile strength ($\sigma_t$) to the following relationship, which considers, in addition to the specimen porosity ($p$), the particle size of the powder ($G$) used to form the compacts:

$$\sigma_t = kG^{-a}e^{-bp} \quad (1)$$

where $a$, $b$ and $k$ are constants. When using the original mean particle size of the fractions in the above equation, only for size fractions 1 and 2 a result could be obtained. For particle size fraction 1, the values of the constants were determined to be 34.9±1.4, 0.2±1.2 and 7.57±0.55 for $k$, $a$ and $b$, respectively (RMS 1.3%, $R^2$=0.997). For particle size fraction 2, the constants found were 39.7±2.5, 0.2±1.5 and 8.5±4.4, respectively (RMS=5.5%, $R^2$=0.860). The term $k\times G^{-a}$ in Eq. 1 represents the zero-porosity tensile strength, which is 18.0 and 17.5 MPa for particle size fractions 1 and 2, respectively. Hence the Knudsen model estimates the zero tensile strength about 3 times that of fraction 2 when using the common exponential relationship (Table 2). An increase in particle size appears to be linked to a slight decrease in the zero tensile strength, which is in agreement with the compact data

Table 3. Volume Specific Surface Area of the Particle Fragments after Compaction ($S_V$; in $cm^2/cm^3$) and Predicted Values of the Particle Fragment Size ($d_f$; in $\mu$m)

| Fraction | | Compaction pressure (MPa) | | | |
|---|---|---|---|---|---|
| | | 75 | 100 | 125 | 150 |
| 1 | $S_V$ | 11564±857 | 14881±1150 | 18496±597 | 21171±344 |
| (20—40 $\mu$m) | $d_f$ | 34.6 | 26.9 | 21.6 | 18.9 |
| 2 | $S_V$ | 8079±269 | 10919±483 | 15441±899 | 15469±896 |
| (40—80 $\mu$m) | $d_f$ | 49.5 | 36.6 | 25.9 | 25.9 |
| 3 | $S_V$ | 1633±131 | 2573±328 | 3488±424 | 3540±148 |
| (250—355 $\mu$m) | $d_f$ | 245.5 | 155.5 | 115.8 | 113.0 |
| 4 | $S_V$ | 1578±24 | 2100±156 | 3025±62 | 3534±112 |
| (355—500 $\mu$m) | $d_f$ | 253.5 | 190.5 | 132.2 | 113.2 |

Values are the arithmetic mean and standard deviation of 3 observations.

provided in Table 1, which also show a tendency for the tensile strength to be less for larger particle size fractions. The decrease in tensile strength of sucrose tablets with an increase in particle size has also been observed by Olsson and Nyström.[5] The observation is in line with fracture mechanics[7] *i.e.* a decrease in particle size increases the fracture toughness of the compacts and the size of the cracks and flaws inherently present in the powder compacts decreases. Thus, more energy is required to break the tablets. The difference between the estimates for the tensile strength at zero porosity reported in Table 2 and for the Knudsen model might be attributed to the fact that the values listed in Table 2 are simply based on an empirical fit of experimental data without any consideration of underlying model assumptions. The Knudsen model, however, assumes that the particle size of the powders does not change during compression. The discrepancy is a first indication that this is an incorrect assumption *i.e.* the sucrose particles fragment under load.

As can be seen, the fit of the data to the model is already poor for particle size fraction 2, and the failure of the model when using the data obtained for particle size fractions 3 and 4 suggests that the larger particles fragment during tabletting and hence the value of $G$ would need to be corrected for the size of the fragments rather than using the original particle size. According to Allen,[14] the particle size is inversely proportional to the specific surface area of the particles. It has been shown that hence the particle size of the fragments $d_f$ after compaction can be estimated from[5]:

$$d_f = \frac{\alpha_{SV}}{S_V} \quad (2)$$

where $\alpha_{SV}$ is the Heywood surface to volume shape factor,[15] and $S_V$ is the volume specific surface area of the powder fragments. The latter values and the predicted size values for the particle fragments are listed in Table 3. Employing Eq. 2 to estimate the $G$-values needed for Eq. 1, the Knudsen model resulted in a very good fit for all four particle size fractions (RMS<2%, $R^2$>0.98), see Fig. 1. In addition, it was possible to pool all values regardless their particle size fraction, and the constants for this overall equation are 17.9±5.0 ($k$), 0.51±0.04 ($a$) and 5.2±0.8 ($b$); RMS=2.0%, $R^2$=0.934. However, as here the $G$-value is variable with compact porosity it is not possible to obtain an estimate for the zero-porosity tensile strength. The approach, however, confirms that extensive fragmentation took place during the compaction process.

**Fracture Mechanics Evaluation** In order to evaluate the influence of pore size, particle size and overall porosity on the tensile strength of the tablets, the critical stress intensity factor in mode I loading[7] was determined for each individual particle size. The minimum crack depth to control the process of crack propagation was determined as described by Podczeck[8] and was found to be 800 $\mu$m. The crack depth used for the determination of the critical stress intensity factor as a function of compact porosity was in all cases between 850 and 900 $\mu$m, thus above this critical threshold value. The extrapolated values for the critical stress intensity factor at zero porosity are listed in Table 2. The magnitude of these values is in agreement with literature data for a particle size of 74 $\mu$m (0.22 MPa $m^{0.5}$; ref. 16). However, as can be seen from the data provided in Table 2, there is apparently an influence of particle size on the values obtained, which is in agreement with findings by Rice[17] on ceramics specimens. While the values for the critical stress intensity factor for particle size fractions 2 to 4 are similar, for the smallest particle size fraction (*i.e.* fraction 1) the zero porosity value is about twice that of the other particle size fractions. This could mean that the critical particle size for fragmentation to occur during compaction is about 20—40 $\mu$m. Hence, there would be only limited particle fragmentation for the smallest particle size fractions, but more or less pronounced particle fragmentation for all other particle size fractions. This is in agreement with the size estimates for the fragments provided in Table 3. The different fragmentation propensity could result in a different crack and flaw pattern inside the compacts and therefore in a different value of the critical stress intensity factor. Roberts and Rowe[18] reported that sucrose particles larger than 30 $\mu$m exhibited extensive fragmentation during compaction, while no fragmentation was observed for particles less than 20 $\mu$m. This is also in agreement with the above findings.

In order to establish a relationship between the fracture mechanics data obtained from beam bending specimens and the strength data obtained from disk shaped tablets, the median pore size of the individual beams was extrapolated from the pore size-porosity relationships obtained on the disks. (The median pore size as a function of the disk porosity could be modelled with a RMS of less than 1% and a $R^2$ of ≥0.99 for all four particle size distributions.)

The Griffith theory[19] relates the tensile strength of a speci-

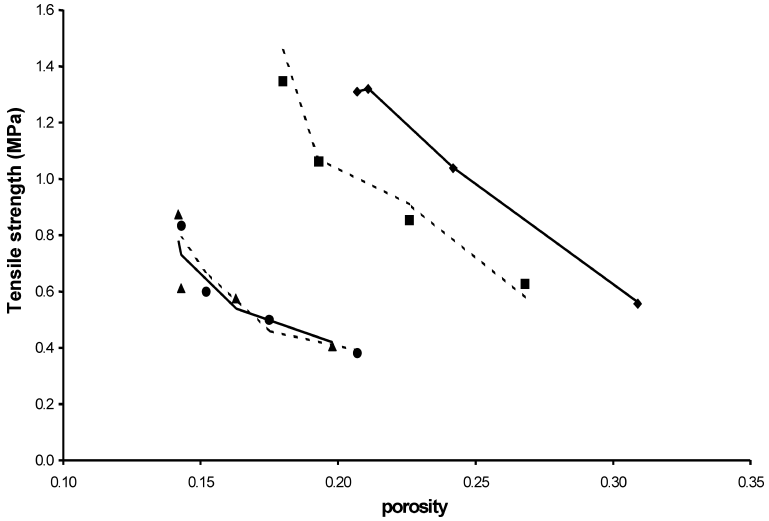


Fig. 1. Tensile Strength of Circular Disk Specimens as a Function of Porosity: Comparison between Experimental and Model Data According to Eq. 1

◆, fraction 1 (20—40 $\mu$m; model data=solid line); ■, fraction 2 (40—80 $\mu$m; model data=dashed line); ▲, fraction 3 (250—355 $\mu$m; model data=solid line); ●, fraction 4 (355—500 $\mu$m; model data=dashed line).

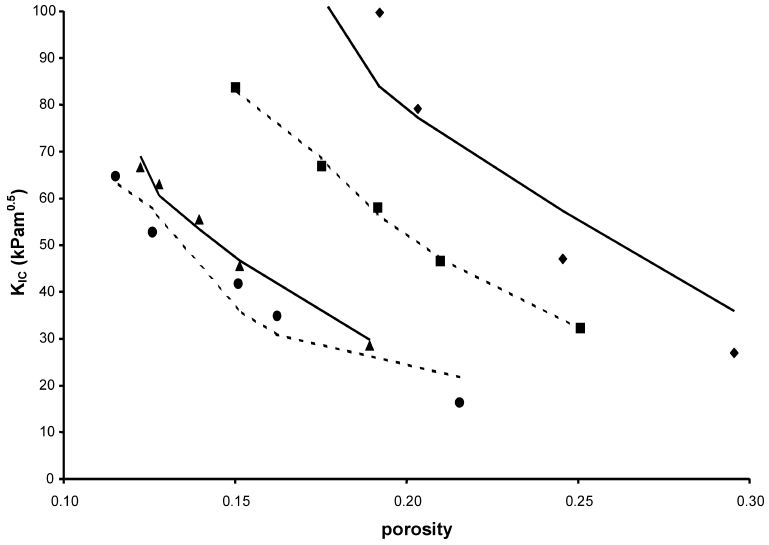


Fig. 2. Critical Stress Intensity Factor as a Function of Beam Porosity: Comparison between Experimental and Model Data According to Eq. 3

◆, fraction 1 (20—40 $\mu$m; model data=solid line); ■, fraction 2 (40—80 $\mu$m; model data=dashed line); ▲, fraction 3 (250—355 $\mu$m; model data=solid line); ●, fraction 4 (355—500 $\mu$m; model data=dashed line).

men solely to the length of a crack that propagates under load assuming that the specimen behaves as an elastic continuum.[20] However, the role of pores in the process of crack propagation needs also consideration. Pores can, under certain circumstances act as a sharp crack, but in most instances their role is that of a stress concentrator only.[21] Ouchiyama *et al.*[22] suggested that the critical stress intensity factor could be related to the crack length and the pore size of the specimen by:

$$K_{IC} = -\left(\frac{a}{r_p}\right)^{0.5} + \frac{b}{\left(1+\left(\frac{a}{r_p}\right)\right)^{c}} \sigma_t (\pi r_p)^{0.5} \quad (3)$$

where $a$ is the crack length, $r_p$ is the pore size, $\sigma_t$ is the tensile strength, and $b$ and $c$ are constants. Employing this model to each individual particle size fraction resulted in very good fit of the model for particle size fractions 2 and 3 ($R^2>0.98$, RMS$<2\%$), and a slightly less fitting result for particle size fraction 4 ($R^2=0.923$, RMS$=10.0\%$). However, for particle size fraction 1 the model fit was less satisfactory ($R^2=0.899$, RMS$=21.7\%$). Figure 2 shows the experimental data and the model functions for all four particle size fractions. The crack lengths $a$ obtained from this model were 86.8, 10.0, 30.2 and 44.0 $\mu$m for particle size fractions 1, 2, 3 and 4, respectively. As observed for the critical stress intensity factor at zero porosity, the estimated crack length for particle size fraction 1 is clearly different from those obtained for the other 3 particle size fractions. While for particle size fraction 1 the calculated crack length is between 2 and 4 times that of the particle size, for all other particle size fractions the crack lengths are less then the length of an individual particle or particle fragment. However, in any case the

crack lengths are significantly larger than the median and the maximum pore sizes measured (see Table 1). Thus, for sucrose specimens, the pores act as stress concentrators, not as sharp cracks. The cracks might be the result of elastic recovery after tablet ejection, which is in excess of 10%,[23] in particular as the estimated crack length is much larger for particle size fraction 1. The specimens of this fraction have larger porosity values and could not be further densified due to excessive elastic expansion after removal from the die. Bortzmeyer *et al.*[24] also reported that the crack lengths of compacted powder specimens—here ceramics powders—was not related to the pore size distributions. These authors determined crack lengths of a size intermediate between particle size and specimen size.

Irwin[25] described the relationship between specimen tensile strength ($\sigma_t$), critical stress intensity factor ($K_{IC}$) and crack length ($a$) as follows:

$$\sigma_t = \frac{K_{IC}}{\sqrt{\pi a}} \tag{4}$$

This equation can be used in two ways to study the relationship between the fracture mechanics approach and the strength of the cylindrical disk specimens. First, the equation can be solved for the crack length using extrapolated data for the critical stress intensity factor at the various porosity values. In this case the crack length was estimated to be 951, 697, 1566 and 1054 $\mu$m for particle fractions 1, 2, 3 and 4, respectively. Under the assumption that some particles did not fragment during tabletting, this would predict a crack along grain boundaries of about 3 original particles when studying particle size fractions 3 and 4. For particle size fractions 1 and 2, however, the predicted flaw sizes appear rather large, being up to 20 times the value of an individual original particle. The propagating cracks could hence be larger flaws formed due to rapid and excessive expansion after tablet ejection. The crack lengths estimated by this approach are much larger than those estimated using Eq. 3. This is not surprising, because Eq. 4 represents a less complex model, which does not consider the pore size of the compacts. In the second approach, the crack length estimated on the basis of Eq. 3 could be used to predict the tablet strength of the cylindrical disks. The strength values obtained by this approach are generally larger than the experimental values. The latter are overestimated by a factor of 3, 8, 7 and 5 for particle fractions 1, 2, 3 and 4, respectively. One conclusion could, therefore, be that Eq. 3 is superior to Eq. 4 in analysing the fracture mechanics of powder compacts. It has to be borne in mind, however, that the geometry and size of the specimens to evaluate the critical stress intensity factor (rectangular beams) and the tensile strength (circular disks) were different. As the compacts were made by uniaxial compression, the stress distribution during compaction will have been different when producing these compacts, and hence, it is likely that different crack and flaw patterns resulted in the process. The overestimation of the crack length or the tensile strength might hence be a representation of differences in the making of these powder compacts. It appears hence necessary to use similar sizes and types of powder compacts when attempting to predict fracture mechanics properties, in particular, as previous work has shown that Eq. 4 can predict the crack size of rectangular specimens correctly if all parameters were obtained from similar powder compacts.[8]

## Conclusions

For powder compacts made from sucrose, the pores themselves are not acting as sharp cracks to initiate failure of these specimens during loading. Instead, they act as stress concentrators. The critical crack length for crack propagation to occur is intermediate between particle and specimen size. For sucrose compacts, crack propagation hence proceeds most likely along grain boundaries.

**Acknowledgements** H.O. is grateful to the ULLA Consortium for financial support to undertake this study. The authors are grateful to Professor J. M. Newton, The School of Pharmacy, University of London (U.K.), for his encouragement to undertake this study and for his proof-reading as native English speaker.

**References**

1) Davies P. N., Newton J. M., "Pharmaceutical Powder Compaction Technology," ed. by Alderborn G., Nyström C., Marcel Dekker, New York, 1995, pp. 165—191.
2) Carneiro F. F. L., Barcellos A., *RILEM Bull.*, **18**, 99—107 (1953).
3) Fell J. T., Newton J. M., *J. Pharm. Pharmacol.*, **20**, 657—658 (1968).
4) Fell J. T., Newton J. M., *J. Pharm. Sci.*, **59**, 688—691 (1970).
5) Olsson H., Nyström C., *Pharm. Res.*, **18**, 203—210 (2001).
6) Alderborn G., Pasanen K., Nyström C., *Int. J. Pharm.*, **23**, 79—86 (1985).
7) Brown W. F., Srawley J. E., "ASTM Spec. Tech. Publ. No 410," Am. Soc. Test. & Mat., Philadelphia, 1967.
8) Podczeck F., *J. Mat. Sci.*, **36**, 4687—4693 (2001).
9) Spriggs R. M., *J. Am. Ceram. Soc.*, **44**, 628—629 (1961).
10) Ryshkewitch E., *J. Am. Ceram. Soc.*, **36**, 65—68 (1953).
11) Duckworth W., *J. Am. Ceram. Soc.*, **36**, 69 (1953).
12) Dewey J. M., *J. Appl. Phys.*, **18**, 578—581 (1947).
13) Knudsen F. P., *J. Am. Ceram. Soc.*, **42**, 376—387 (1959).
14) Allen T., "Particle Size Measurement," 5th ed., Vol. 2, Chapman & Hall, London, 1997, pp. 1—4.
15) Heywood H., *J. Pharm. Pharmacol.*, **15**, 56T—74T (1963).
16) Roberts R. J., Rowe R. C., York P., *Int. J. Pharm.*, **91**, 173—182 (1993).
17) Rice R. W., *J. Mat. Sci.*, **31**, 1969—1983 (1996).
18) Roberts R. J., Rowe R. C., *J. Pharm. Pharmacol.*, **52**, 147—150 (2000).
19) Griffith A. A., *Trans. Roy. Soc. Ser. A*, **221**, 163—198 (1920).
20) Kendall K., McN Alford N., Birchall J. D., *Inst. Ceram. Proc. Special Ceramics*, **8**, 255—265 (1986).
21) Rice R. W., *J. Mat. Sci.*, **19**, 895—914 (1984).
22) Ouchiyama N., Benbow J. J., Bridgewater J., *Powder Technol.*, **51**, 103—114 (1987).
23) Olsson H., "Particle Interactions and Internal Tablet Structure," Ph. D. Thesis, Swedish University Press, Ekonomikum, Uppsala, 2000.
24) Bortzmeyer D., Langguth G., Orange G., *J. Eur. Ceram. Soc.*, **11**, 9—16 (1993).
25) Irwin G. R., *J. Appl. Mech.*, **24**, 361—364 (1957).